

Elastic behavior and phase stability of pollucite, a potential host for nuclear waste

G. DIEGO GATTA,^{1,2,*} NICOLA ROTIROTI,^{1,2} TIZIANA BOFFA BALLARAN,³ CARMEN SANCHEZ-VALLE,⁴
AND ALESSANDRO PAVESE^{1,2}

¹Dipartimento di Scienze della Terra, Università degli Studi di Milano, Via Botticelli 23, I-20133 Milano, Italy

²CNR-Istituto per la Dinamica dei Processi Ambientali, 20133 Milano, Italy

³Bayerisches Geoinstitut, Universität Bayreuth, Universitaetsstrasse 30, D-95447 Bayreuth, Germany

⁴Institute for Mineralogy and Petrology, ETH Zürich, Clausiusstrasse 25, H-8092 Zürich, Switzerland

ABSTRACT

The elastic behavior and the phase stability of natural pollucite, $(\text{Cs,Na})_{16}\text{Al}_{16}\text{Si}_{32}\text{O}_{96}\cdot n\text{H}_2\text{O}$, were investigated at hydrostatic pressure by in situ single-crystal X-ray diffraction with a diamond-anvil cell. Pollucite experiences a P -induced phase transition, not previously reported in the literature, at $P = 0.66 \pm 0.12$ GPa from cubic ($Ia\bar{3}d$) to triclinic symmetry ($P\bar{1}$). The phase transition is completely reversible and without any appreciable hysteresis effect. No further phase transition has been observed up to 9 GPa. Fitting the pressure-volume data of the low-pressure cubic polymorph with a second-order Birch-Murnaghan Equation-of-State (BM-EoS), we obtain $V_0 = 2558.3(4)$ Å³, $K_{T0} = 41(2)$ GPa, and $K'_T = 4$ (fixed). For the high-pressure triclinic polymorph, a third-order BM-EoS fit gives $V_0 = 2577.5(40)$ Å³, $K_{T0} = 25.1(9)$ GPa, and $K'_T = 6.5(4)$. The axial bulk moduli of the high-pressure triclinic polymorph were calculated with a third-order “linearized” BM-EoS. The EoS parameters are $a_0 = 13.699(12)$ Å, $K_{T0}(a) = 25.5(17)$ GPa, and $K'_T(a) = 6.8(6)$ for the a axis; $b_0 = 13.728(12)$ Å, $K_{T0}(b) = 23.2(15)$ GPa, and $K'_T(b) = 7.7(7)$ for the b axis; $c_0 = 13.710(7)$ Å, $K_{T0}(c) = 25.2(10)$ GPa, and $K'_T(c) = 6.8(4)$ for the c axis [$K_{T0}(a):K_{T0}(b):K_{T0}(c) = 1.10:1:1.09$]. Brillouin light-scattering was used to investigate the single-crystal elastic properties of pollucite at ambient conditions. The aggregate adiabatic bulk modulus (K_s) and shear modulus (G), calculated using the Voigt-Reuss-Hill averaging procedures, are $K_s = 52.1(10)$ GPa and $G = 31.5(6)$ GPa. The elastic response of pollucite and other isotypic materials (e.g., analcime, leucite, and wairakite) is compared. The high thermo-elastic stability of pollucite, reflected by the preservation of crystallinity at least up to 9 GPa (at room T) and 1470 K (at room P) in elastic regime, the large amount of Cs hosted in this material ($\text{Cs}_2\text{O} \sim 30$ wt%), the immobility of Cs at high-temperature and high-pressure conditions, and the extremely low leaching rate of Cs, make of this open-framework silicate a functional material with potential use for fixation and deposition of Cs radioisotopes in high-level nuclear waste.

Keywords: Pollucite, single-crystal X-ray diffraction, high-pressure, compressibility, phase transition, nuclear waste disposal material

INTRODUCTION

Pollucite is a zeolite mineral (Coombs et al. 1997), although it is commonly defined as a feldspathoid, with ideal formula $(\text{Cs,Na})_{16}\text{Al}_{16}\text{Si}_{32}\text{O}_{96}\cdot n\text{H}_2\text{O}$ (with $\text{Cs} + n = 16$). Pollucite occurs mainly in Li-Cs-rich granitic pegmatites in association with quartz, muscovite, K- and Na-feldspars, spodumene, petalite, lepidolite, elbaite, eucryptite, and apatite.

Pollucite is isotypic with analcime ($\text{Na}_{16}\text{Al}_{16}\text{Si}_{32}\text{O}_{96}\cdot 16\text{H}_2\text{O}$), leucite ($\text{K}_{16}\text{Al}_{16}\text{Si}_{32}\text{O}_{96}$), wairakite ($\text{Ca}_8\text{Al}_{16}\text{Si}_{32}\text{O}_{96}\cdot 16\text{H}_2\text{O}$), and hsianghualite ($\text{Li}_{16}\text{Ca}_{24}\text{Be}_{24}\text{Si}_{24}\text{O}_{96}\text{F}_{16}$) (Gottardi and Galli 1985; Armbruster and Gunter 2001; Baerlocher et al. 2001), and forms a complete solid-solution series with analcime (Černý 1974; Legache 1995; Teertstra and Černý 1995). The (open) tetrahedral framework of this group of isotypic minerals (i.e., the “analcime group”) results from the combination of two “secondary building units” (SBU, Baerlocher et al. 2001), constituted by 4- and 6-membered rings of tetrahedra (ANA topology, Baerlocher et al.

2001) (Fig. 1). The topological symmetry of such a framework type is cubic, with space group $Ia\bar{3}d$ (Baerlocher et al. 2001). At room conditions, the general symmetry of pollucite is cubic $Ia\bar{3}d$, with $a \sim 13.68$ Å. In cubic pollucite, there is a disordered Si/Al-distribution in the tetrahedral framework, with only one independent tetrahedral site (at $x,y,1/8$, Wyckoff position 48g). Cesium, Na, and H_2O represent the extra-framework content. According to the structural model of Beger (1969) (i.e., “model 1”), water molecules and Cs atoms share the only extra-framework site (i.e., Cs/W-site, Fig. 1) lying in the 6-membered ring channels (6mR) along [111] (at $1/8,1/8,1/8$, Wyckoff position 16b), whereas sodium atoms are located out from the 6mR-channels (at $1/4,1/8,0$, Wyckoff position 24c), in the distorted 8-membered ring of tetrahedra that connect the 6mR-channels. Cesium atoms are coordinated by 12 O atoms belonging to the tetrahedral framework (6 Cs-O ~ 3.39 Å and 6 Cs-O ~ 3.56 Å, Beger 1969). The H_2O -molecules and the sodium atoms occupy the same site positions as they do in analcime, but they occur only in randomly distributed clusters of atoms forming interrupted $\cdots[\text{H}_2\text{O}-\text{Na}-\text{H}_2\text{O}]\cdots$ chains, with $\text{H}_2\text{O}/\text{Na} \leq 2$ (Beger 1969). On

* E-mail: diego.gatta@unimi.it

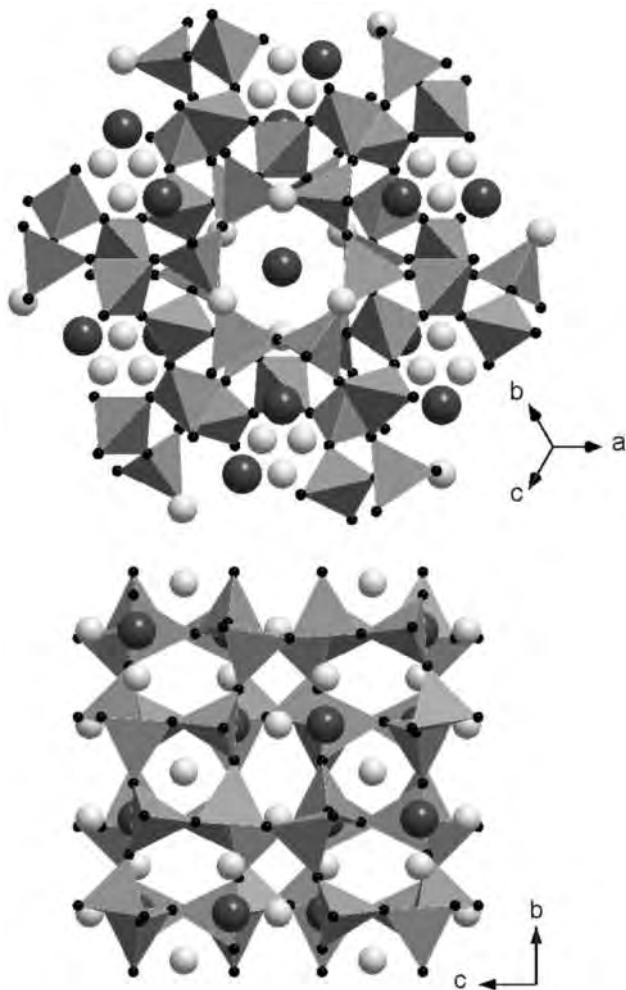


FIGURE 1. Crystal structure of cubic pollucite viewed down [111] (above) and down [100] (below). The large dark-gray spheres represent the Cs/W-sites, the small light-gray spheres the Na-sites.

this basis, in pollucite (Cs + H₂O) sum to 16 apfu, the number of Na atoms is less than the number of H₂O molecules and the total amount of the alkali atoms must be <16 apfu (when the crystal contains water), leading to a general chemical formula: Cs_xNa_yAl_{x+y}Si_{48-x-y}O₉₆ · (16 - x)H₂O, in which 2y ≥ (16 - x) ≥ y. These crystallochemical features are supported by the chemical compositions of pollucite specimens from several localities (Beger 1969). However, Beger (1969) reported also a further possible structural model of pollucite (i.e., “model 2”), in which Cs and Na share the same extra-framework site at 1/8, 1/8, 1/8 (Wyckoff position 16b) and water lies at 1/4, 1/8, 0 (Wyckoff position 24c). However, crystallochemical arguments led the author to suggest “model 1” as the most reliable. The structural “model 1” of Beger (1969), and in particular the configuration of the extra-framework content, is consistent with the previous structural description of Náráay-Szabó (1938), with the dehydration behavior provided by Fleischer and Ksanda (1940), and with the experimental findings of Newnham (1967) based on the near-infrared absorption spectrum of pollucite. The amount of water in pollucite is lower than in other zeolites, ranging

between 0–4 wt%. The dehydration experiments on natural pollucites showed no loss in weight below 573 K, with a completely dehydrated form at 913 K (Fleischer and Ksanda 1940). Unlike typical zeolites, after dehydration pollucites did not take up water on exposure to air saturated with water vapor. Deviations from cubic to tetragonal symmetry (at room conditions) have been reported by Palmer et al. (1997) (with $c/a = 1.0051$) and Xu et al. (2002) (with $c/a = 1.0014$) for synthetic Cs₁₆Al₁₆Si₃₂O₉₆ by powder diffraction experiments.

Despite its microporous structure, pollucite is currently considered a “ceramic” material (Kobayashi et al. 1997 and references therein), with potential technological applications. Pollucite is able to retain Cs when immersed in a fluid phase, even under hydrothermal conditions, better than several other Cs-bearing zeolites. This behavior is ascribable to the topological configuration of the Cs-polyhedron and its bonding environment, to the small dimensions of the sub-nanopores where the Cs-sites lie and to the high flexibility of the ANA framework type (Gatta 2008; Gatta et al. 2006, 2008a), which lead to better thermo-elastic stability of pollucite compared to other synthetic microporous and mesoporous Cs-aluminosilicates. In this light, pollucite can be considered as a functional material potentially usable for fixation and deposition of radioactive isotopes of Cs (Richerson and Hummel 1972; Gallagher et al. 1977; Komameni and White 1981; Yanagisawa et al. 1987; Mimura et al. 1990; Kobayashi et al. 1997, 2006; Yanase et al. 1997; Gatta et al. 2008b).

Because of its potential technological applications, the high- and low-temperature crystal chemistry of pollucite has been investigated extensively (Fleischer and Ksanda 1940; Taylor and Henderson 1968; Kobayashi et al. 1997, 2006; Palmer et al. 1997; Yanase et al. 1997; Ogorodova et al. 2003; Xu et al. 2002). Kobayashi et al. (1997) reported that synthetic cubic pollucite (Cs₁₆Al₁₆Si₃₂O₉₆) preserves its crystallinity at least up to 1470 K (at room *P*), without any evidence of phase transition between 290 and 1470 K. Yanase et al. (1997) investigated the low-temperature behavior of synthetic Cs₁₆Al₁₆Si₃₂O₉₆ between 93 and 298 K (at room *P*), and found a low-temperature displacive phase transition from *Ia* $\bar{3}d$ to *I4*₁/*acd* symmetry at about 265 K. By contrast, the elastic behavior of pollucite and its structural evolution under pressure are completely unknown. The aim of this study is to investigate the high-*P* behavior of pollucite by in situ single-crystal X-ray diffraction with a diamond-anvil cell under hydrostatic regime. A comparison between the elastic response of pollucite and that of isotopic materials (e.g., analcime, leucite, and wairakite) is also made.

EXPERIMENTAL METHODS

A sample of natural pollucite from Greenwood, Oxford County, Maine, was used for the high-pressure experiment. Quantitative chemical analyses in EMPA-WDS mode were performed on a polished single crystal (300 × 250 × 200 μm), optically free of inclusions, using a Jeol JXA-8200 electron microprobe at the laboratory of the Earth Sciences Department, University of Milan. The system was operated using a defocused electron beam (∅ 10 μm) at an accelerating voltage of 15 kV, a beam current of 15 nA, and counting times of 20 s on the peaks and 5 s on the backgrounds. A series of natural minerals (K-feldspar for Si, K, Al; pollucite for Cs and Rb; wollastonite for Ca; omphacite for Na; and fayalite for Fe) were employed as standards. The results were corrected for matrix effects using a conventional ZAF routine in the Jeol suite of programs. The crystal was found to be homogeneous within analytical error. The chemical composition (obtained by averaging 10 point analyses) is: Cs₂O 34.61 wt%, Rb₂O 0.71 wt%, K₂O 0.06 wt%, Na₂O 1.26 wt%,

CaO <0.01 wt%, Fe₂O₃ <0.01 wt%, Al₂O₃ 14.06 wt%, SiO₂ 47.76 wt%, and H₂O 1.54 wt% (by difference). The chemical formula, on the basis of 96 oxygen atoms, is (Cs_{10.976}Rb_{0.352}K_{0.064}Na_{1.824})_{Σ=13.216}(Al_{12.304}Si_{13.472})_{Σ=47.776}O₉₆ · 3.79H₂O.

A transparent, colorless, platy crystal of pollucite (190 × 130 × 60 μm³) from the same natural sample analyzed in EMPA-WDS, optically free of defects, twinning or inclusions, and with isotropic extinction in transmitted polarized light, was selected for the X-ray diffraction experiments. Accurate lattice parameters were determined with a KUMA-KM4 diffractometer, equipped with a point-detector and monochromatized MoK α -radiation, on the basis of 36 Bragg reflections. Pollucite was found to be metrically cubic, with $a = 13.667(1)$ Å. Diffraction intensity data were collected at room conditions adopting the data collection strategy reported in Table 1, without any symmetry restraint. The diffractometer was operated at 50 kV and 40 mA. The reflection conditions were consistent with space group $Ia\bar{3}d$. Integrated intensity data were corrected for Lp and absorption effects using the ABSORB5.2 computer program (Burnham 1966; Angel 2002, 2003). The anisotropic structure refinement against F^2 was then performed using the SHELX-97 software (Sheldrick 1997), starting from the atomic coordinates of the structural “model 1” of Beger (1969). Only the Na-site was maintained isotropic because of the low site occupancy. Neutral atomic scattering factors of Cs, Na, Si, and O from the *International Tables for Crystallography* (Wilson and Prince 1999) were used (i.e., a H-free structure was considered). A mixed scattering curve was used for the Cs/W-site, partially occupied by cesium and oxygen (of the water molecule), with (%Cs + %O_w) = 100%. A scattering curve based on partially occupied tetra-

hedral sites (by Al and Si) and the use of ionic curve for all the atomic sites did not improve significantly the figures of merit of the refinement. The convergence was rapidly achieved after a few cycles of refinement. At the end of the refinement, the variance-covariance matrix did not show any significant correlation among the refined parameters. No peak larger than $\pm 0.27 e^{-}/\text{Å}^3$ was present in the final difference Fourier synthesis and $R_1(F) \sim 0.02$ for 22 refined parameters. Further details of the structure refinement are reported in Table 1. Refined atomic positions, site occupancies, atomic displacement parameters, bond distances, and angles are listed in Table 2.

A diamond anvil cell (DAC) designed by Miletich et al. (2000) (ETH-type DAC) was used for the high-pressure experiments at room T . Steel T301 foil (250 μm thick) was used as gasket. The gasket foil was pre-indent to a thickness of about 115(2) μm before drilling a micro-hole (\emptyset 350 μm) by spark-erosion. The crystal of pollucite previously studied at room conditions was placed into the gasket hole together with a few ruby chips used for the pressure calibration (Mao et al. 1986). A methanol:ethanol:water (16:3:1) mixture was used as a hydrostatic pressure-transmitting medium (Angel et al. 2007). Accurate lattice parameters were measured up to about 8.8 GPa (Table 3) with a Huber four-circle diffractometer (non-monochromatized MoK α radiation) using eight-position centering of 21 Bragg reflections, according to the protocol of King and Finger (1979) and Angel et al. (2000).

RESULTS

Crystal-structure of pollucite at ambient conditions

At ambient conditions (i.e., 0.0001 GPa and 293 K), the diffraction pattern of the natural pollucite shows a metrically cubic unit cell [the deviation from isometry is $<1.5\sigma(l_i)$, where l_i are the unrestrained unit-cell lengths] and the reflection conditions are consistent with the space group $Ia\bar{3}d$. The anisotropic structure refinement confirms the “model 1” of Beger (1969) in which cesium and oxygen (of water molecules) share the same extra-framework site lying in the 6mR-channel at 1/8, 1/8, 1/8 (Fig. 1; Table 2), whereas sodium lies out from the 6mR-channel at 1/4, 1/8, 0 (Fig. 1; Table 2). With this configuration, the coordination shell of the Cs-site consists of 12 O atoms belonging to the tetrahedral framework, with six Cs-O bond distances of about 3.397 Å and six of about 3.555 Å (Table 2). The Na-site is bonded to four O atoms belonging to the tetrahedral framework (with Na-O of about 2.500 Å) and two water molecules (with Na-W of about 2.416 Å) (Table 2). The refined bond distances and angles of the tetrahedron are consistent with a disordered Si/Al-distribution in the tetrahedral framework (with $\langle T-O \rangle = 1.6365$, Table 2). The “free diameter” (Baerlocher et al. 2001) of the 6mR-channel along [111] is only ~ 2.86 Å (Table 2). The crystal formula derived from the structure refinement is:

TABLE 1. Details pertaining to the data collection and structure refinement of cubic pollucite at ambient conditions

Crystal size (μm ³)	190 × 130 × 60
a (Å)	13.667(1)
Space group	$Ia\bar{3}d$
T (K)	298
P (GPa)	0.0001
ρ_s (g/cm ³) (H-free structure)	2.819
Radiation	MoK α
μ (mm ⁻¹)	4.45
Detector type	Point-detector
2 θ range (°)	2–60
Scan type	ω
Scan speed (°/s)	0.02
Scan width (°)	1.4
No. measured reflections	4026
No. unique reflections	304
No. unique reflections with $F_o > 4\sigma(F_o)$	194
No. refined parameters	22
R_{int}	0.102
R_σ	0.037
$R_1(F)$ with $F_o > 4\sigma(F_o)$	0.021
$R_1(F)$ with all the reflections	0.068
$wR_2(F^2)$	0.057
GooF	1.094
Residuals ($e^{-}/\text{Å}^3$)	+0.27/−0.27

Notes: Standard deviations are in parentheses. $R_{int} = \sum |F_o^2 - F_c^2(\text{mean})| / \sum F_o^2$; $R_\sigma = \sum (\sigma(F_o^2)) / \sum F_o^2$; $R_1 = \sum (|F_o| - |F_c|) / \sum |F_o|$; $wR_2 = \{ \sum [w(F_o^2 - F_c^2)^2] / \sum [w(F_o^2)^2] \}^{0.5}$.

TABLE 2. Refined atomic positions, displacement parameters (Å²), and relevant bond distances (Å) and angles (°) of cubic pollucite at ambient conditions

Site	x	y	z	Site occupancy	U_{11}	U_{22}	U_{33}	U_{23}	U_{13}	U_{12}	U_{iso}/U_{eq}
Cs/W (16b)	1/8	1/8	1/8	0.670(6) Cs 0.330(6) Ow	0.0348(3)			0.0040(2)			0.0348(3)
Na (24c)	1/4	1/8	0	0.068(8)							0.022(9)
T (48g)	1/8	0.66217(5)	0.58783(5)	1	0.0144(5)	0.0156(4)		−0.0022(4)	0.0025(3)		0.0152(4)
O (96h)	0.1047(2)	0.1336(2)	0.7196(2)	1	0.049(2)	0.045(1)	0.025(1)	0.0022(9)	0.0100(9)	0.009(1)	0.0402(9)
Cs/W-Na	2.4160										
Cs-O ⁱ (×6)	3.397(2)		T-O-T ⁱ	106.5(2)							
Cs-O ⁱⁱ (×6)	3.555(2)		T-O-T ⁱⁱ	111.3(2)							
Na-O (×4)	2.500(2)		T-O-T ⁱⁱⁱ	111.5(1)							
			T-O-T ^{iv}	104.9(2)							
T-O ⁱ (×2)	1.636(2)										
T-O ⁱⁱ (×2)	1.637(2)		O ↔ O _{6mR}}	2.86							
<T-O>	1.6365										

Note: Standard deviations are in parentheses. For the Cs/W-site, the scattering curve of Cs and O were used and the refined site occupancies of the two elements are given; for the T-site, the scattering curve of Si alone was used. Na-site was the only one refined isotropically, because of the low site occupancy, and the U_{iso} value is given. O ↔ O_{6mR}} is the “free diameter” of the 6mR-channel along [111] (Baerlocher et al. 2001).

TABLE 3. Unit-cell parameters of pollucite at different pressures

<i>P</i> (GPa)	<i>a</i> (Å)	<i>b</i> (Å)	<i>c</i> (Å)	α (°)	β (°)	γ (°)	<i>V</i> (Å ³)
0.0001*	13.6767(8)	–	–	–	–	–	2558.3(4)
0.25(3)	13.6510(8)	–	–	–	–	–	2543.9(5)
0.46(3)	13.6262(9)	–	–	–	–	–	2530.0(6)
0.54(4)	13.6176(9)	–	–	–	–	–	2525.2(5)
0.79(3)	13.5714(26)	13.5909(26)	13.5800(15)	90.194(24)	89.821(22)	89.772(16)	2504.7(7)
1.01(3)	13.5407(17)	13.5538(19)	13.5512(13)	90.331(13)	89.678(10)	89.631(11)	2486.9(5)
2.24(4)	13.3741(43)	13.4047(37)	13.3877(33)	90.924(40)	89.064(37)	88.997(25)	2399.1(12)
3.70(3)	13.2461(35)	13.2464(33)	13.2458(22)	91.472(26)	88.519(24)	88.495(21)	2321.8(9)
4.54(3)	13.1621(29)	13.1746(33)	13.1703(19)	91.731(20)	88.279(18)	88.205(19)	2280.5(8)
5.52(3)	13.0883(30)	13.0929(27)	13.0913(20)	91.968(23)	88.025(22)	87.941(18)	2239.2(8)
7.28(3)	12.9671(29)	12.9803(25)	12.9736(24)	92.378(24)	87.633(22)	87.550(17)	2177.8(8)
8.79(5)	12.8748(50)	12.8848(47)	12.8765(27)	92.702(35)	87.311(35)	87.238(31)	2128.6(12)

Notes: The phase transition from cubic to triclinic polymorph occurs at ~0.66 GPa. Standard deviations are given in parentheses.

* Data with the crystal in the DAC without any *P*-medium.

$\text{Cs}_{1.72}\text{Na}_{1.59}(\text{Al},\text{Si})_{48}\text{O}_{96} \cdot 5.28\text{H}_2\text{O}$. Any attempt to refine the crystal structure of pollucite either on the basis of “model 2” of Beger (1969) or decreasing the symmetry to tetragonal, as reported for synthetic $\text{Cs}_{16}\text{Al}_{16}\text{Si}_{32}\text{O}_{96}$ by Palmer et al. (1997) and Xu et al. (2002) from powder diffraction experiments (i.e., I_{41}/a , with $c > a$), led to a worsening of the figures of merit.

Elastic behavior and phase stability

Evolution of the unit-cell parameters of pollucite with pressure is shown in Figure 2. A phase transition from cubic to triclinic structure was observed in the pressure range 0.54 to 0.78 GPa. The transition pressure was bracketed by several X-ray diffraction measurements and in transmitted polarized light microscopy, in both compression and decompression experiments. The phase transition is either very weakly first-order or continuous in character, as shown in Figure 2. The transition is reversible and without any appreciable hysteresis effect (if hysteresis occurs, the loop is <0.12 GPa). The high-*P* polymorph shows a metrically triclinic unit cell, as the result of slight distortion of the low-*P* cubic structure, with $a \sim b \sim c$ and $\alpha > \beta \sim \gamma$ (Table 3). This lattice set is consistent with that already used to describe the high-*P* polymorph of leucite (Gatta et al. 2008a). The evolution of the unit-cell parameters with *P* of the HP triclinic polymorph is continuous and monotonic up to 8.8 GPa, without any evidence of a further phase transition or anomalous elastic behavior within the *P*-range investigated.

The *P*-*V* data of the low-*P* cubic polymorph were fitted with a truncated second-order Birch-Murnaghan Equation-of-State (BM-EoS) (Birch 1947; Angel 2000), using the EOS-FIT5.2 computer program (Angel 2001). The fitting process was performed using data weighted by uncertainties in *P*-*V*. The refined EoS parameters are $V_0 = 2558.3(4) \text{ \AA}^3$, $K_{T0} = 41(2) \text{ GPa}$, and $K'_T = 4$ (fixed).

For the high-*P* triclinic polymorph, a weighted fit of the *P*-*V* data with a third-order BM-EoS yields $V_0 = 2577.5(40) \text{ \AA}^3$, $K_{T0} = 25.1(9) \text{ GPa}$, and $K'_T = 6.5(4)$. The confidence ellipse at 68.3% level (1σ , $\Delta\chi^2 = 2.30$) was calculated starting from the variance-covariance matrix of K_{T0} and K'_T obtained from the BM-EoS least-square procedure for the HP triclinic polymorph. The ellipse is elongated with a negative correlation of K_{T0} vs. K'_T (Fig. 3). The individual values for K_{T0} and K'_T are $25.1 \pm 1.5 \text{ GPa}$ and 6.5 ± 0.6 , respectively (Fig. 3).

The Eulerian finite strain, i.e., $f_e = [(V_0/V)^{2/3} - 1]/2$, vs. normalized stress, i.e., $F_e = P/[3f(1 + 2f)^{5/2}]$, plots for the low- and

high-*P* polymorphs were calculated and shown in Figure 4. For the HP triclinic polymorph, the theoretical V_0 value used for the Eulerian strain calculation was that refined by the third-order BM-EoS fit. The weighted linear regression through the data points pertaining to the HP polymorph yields the intercept value $F_e(0) = 25.1(2) \text{ GPa}$. The slope of the regression line leads to $K'_T = 6.5(2)$ (Angel 2000).

The axial bulk moduli of the HP triclinic polymorph were calculated with a third-order “linearized” BM-EoS (Angel 2000). The EoS parameters are $a_0 = 13.699(12) \text{ \AA}$, $K_{T0}(a) = 25.5(17) \text{ GPa}$, and $K'_T(a) = 6.8(6)$ for the *a* axis; $b_0 = 13.728(12) \text{ \AA}$, $K_{T0}(b) = 23.2(15) \text{ GPa}$, and $K'_T(b) = 7.7(7)$ for the *b* axis; $c_0 = 13.710(7) \text{ \AA}$, $K_{T0}(c) = 25.2(10) \text{ GPa}$, and $K'_T(c) = 6.8(4)$ for the *c* axis [$K_{T0}(a):K_{T0}(b):K_{T0}(c) = 1.10:1:1.09$]. The axial compressibility coefficients and the “linearized” bulk moduli are related by $K_{T0j} = -1/(3\beta_j)$, where β_j is the axial compressibility coefficient ($\beta_j = l_j^{-1} \partial l/\partial P$) (Angel 2000).

The limited portion of reciprocal space accessible at high pressure, together with the low quality of the diffraction data at pressures above the cubic-to-triclinic phase transition and the high number of independent parameters to describe the triclinic structure (Gatta et al. 2006, 2008a), did not allow solution and refinement of the crystal structure of the HP triclinic polymorph. However, the presence of a relevant number of $(h + k + l) \neq 2n$ reflections, violating the body-centered symmetry, suggests that the space group of the triclinic polymorph is $P\bar{1}$.

As the cubic-to-triclinic phase transition occurs at very low *P*, the calculation of the elastic properties of cubic pollucite based on in situ diffraction data are hindered by the limited *P*-range investigated. Therefore, a further experiment was performed by Brillouin scattering spectroscopy. Brillouin scattering is a non-destructive technique for investigating the elastic properties of small single crystals, allowing direct measurement of the sound velocity along general directions in a transparent medium and hence the determination of the elastic stiffness tensor C_{ij} , as well as aggregate properties (Musgrave 1970; Nye 1985 and references therein). This technique has been recently applied to investigate the elastic properties of various zeolites, including analcime (Sanchez-Valle et al. 2005, 2008). Phonon velocities are related to the single-crystal elastic moduli through Christoffel’s equation (Nye 1985). Pollucite is cubic and has only three independent elastic constants (i.e., C_{11} , C_{44} , and C_{12}), which can be obtained by measuring the acoustic velocities in a few non-equivalent crystallographic directions in a single crystallographic

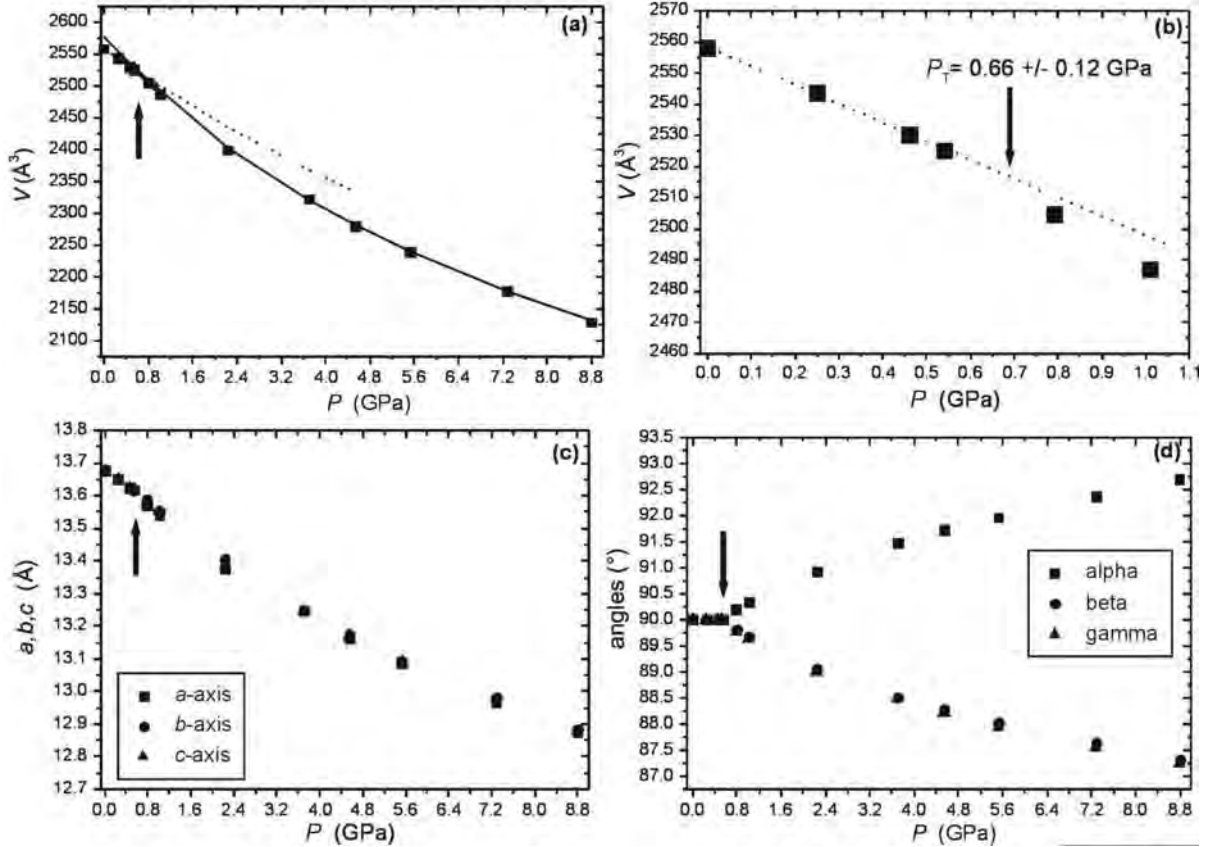


FIGURE 2. Evolution of the unit-cell volume (**a**, **b**), lengths (**c**), and angles (**d**) of pollucite as a function of P and BM-EoS-fit for cubic (dotted line) and triclinic (solid line) polymorphs. The black arrows represent the transition pressure (P_T) from cubic to triclinic polymorph. The e.s.d. values are slightly smaller than the size of the symbols.

plane. We conducted multiple acoustic velocity measurements in two different sample platelets prepared from the same sample used for the previous X-ray diffraction experiment. Brillouin scattering measurements were conducted using a solid state Nd:YVO₄ laser ($\lambda_0 = 532.1$ nm) as excitation source, a 6-pass tandem Fabry-Perot interferometer to analyze the scattered light (Sandercock 1982) and a photomultiplier tube for collection. The power of the focused beam was kept below 20 mW at the sample to prevent damage or dehydration of the samples. Experiments were performed in symmetric (platelet) scattering geometry with an external scattering angle (i.e., angle between the incident and scattered light outside the sample plate) of 90°. The orientation of the two sample platelets was refined using the collected velocity data and is given by the normal vectors (0.616, 0.435, 0.657) and (0.574, 0.466, 0.674), respectively. The phonon directions, determined with a precision better than 3°, and the measured acoustic velocities were then used as input data to a linearized inversion procedure to solve for the independent elastic constants. Inversion of the acoustic velocity data set obtained from both samples provides the following C_{ij} values for our pollucite specimen: $C_{11} = 105.0(13)$, $C_{44} = 27.0(3)$, and $C_{12} = 25.7(5)$ GPa. The aggregate adiabatic bulk modulus (K_s), shear modulus (G), and aggregate acoustic velocities were calculated from the C_{ij} values using the Voigt-Reuss-Hill averaging procedures: $K_s = 52.1(10)$ GPa, $G = 31.5(6)$ GPa, $v_p = 5.67(8)$ km/s, and $v_s = 3.28(4)$ km/s. The aggregate Poisson's ratio (ν) and the Young's modulus (E) are $\nu = 0.248(4)$ and $E = 78.6(13)$ GPa, respectively. Further

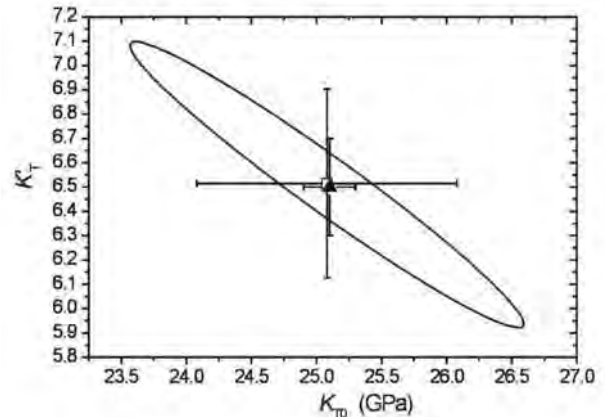


FIGURE 3. Confidence ellipse at the 68.3% level (1σ , $\Delta\chi^2 = 2.30$) in K_{T0} and K_{T1} for the fit of third-order BM-EoS to the triclinic polymorph P - V data. The BM-EoS K_{T0} and K_{T1} (square) and the co-respective parameters calculated with the fe - Fe plot [$Fe_v(0)$ and K_T^* , triangle] are shown. Error bars are ± 1 e.s.d.

details pertaining to the Brillouin experiment on pollucite will be published elsewhere in a more extensive form.

DISCUSSION AND CONCLUDING REMARKS

Pollucite shows a previously unreported phase transition at $P_T = 0.66 \pm 0.12$ GPa from cubic ($Ia\bar{3}d$) to triclinic symmetry ($P\bar{1}$). This phase transition results in a slight distortion of the structure, as shown by the unit-cell parameters above and below the transi-

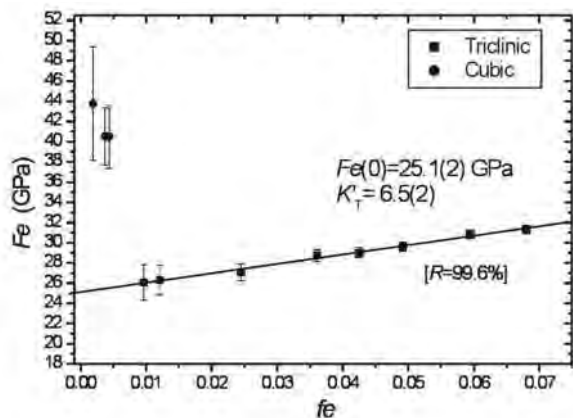


FIGURE 4. Plot of the Eulerian finite strain (f_e) vs. the normalized stress (F_e) for cubic and triclinic pollucite. The e.s.d. values were calculated according to Angel (2000). The weighted linear regression through the data points of the high-pressure triclinic polymorph is shown.

tion pressure (Table 3). On the basis of the structural homologies between pollucite and analcime ($\text{Na}_{16}\text{Al}_{16}\text{Si}_{32}\text{O}_{96} \cdot 16\text{H}_2\text{O}$), we suggest that the P -induced phase transition in pollucite is displacive in character. Analcime undergoes a $Ia\bar{3}d \rightarrow P\bar{1}$ first-order phase transition at about 1 GPa (Gatta et al. 2006; Gatta 2008). Structure refinements of the cubic and triclinic polymorphs of analcime show that the P -induced phase transition is displacive, leading to a slight distortion of the tetrahedral framework (by tilting of the Si/Al-tetrahedra) maintaining the topology of the high-symmetry phase. P -induced high-symmetry to low-symmetry phase transitions occur in all the isotypic members of the “analcime-group.” Leucite ($\text{K}_{16}\text{Al}_{16}\text{Si}_{32}\text{O}_{96}$) undergoes a first-order phase transition from tetragonal to triclinic symmetry ($I4_1/a \rightarrow P\bar{1}$) at about 2.4 GPa, with a drastic increase in density ($\sim 4.7\%$) (Gatta et al. 2008a). A similar high- P behavior was also observed in wairakite ($\text{Ca}_8\text{Al}_{16}\text{Si}_{32}\text{O}_{96} \cdot 16\text{H}_2\text{O}$), where a phase transition from monoclinic to triclinic ($I2/a \rightarrow P\bar{1}$) structure occurs at ~ 2.5 GPa (Ori et al. 2008). P -induced phase transitions due to an over-hydration effect (through selective sorption of water molecules from the pressure medium) do not occur in all the isotypic zeolites with ANA framework type because of the small “free diameter” of the $6\text{mR}[111]$ -channels ($\text{O} \leftrightarrow \text{O}_{6\text{mR}}$, Table 2) and of the configuration of the extra-framework content (Gatta et al. 2005; Gatta 2008).

As for analcime, leucite, and wairakite, we observe that the high- P polymorph of pollucite is more compressible than the low- P one. However, in leucite, wairakite, and pollucite, the difference between the isothermal bulk moduli of the two P -polymorphs [i.e., $K_{\text{T0}}(\text{tetragonal leucite}) = 41.9(6)$ GPa and $K_{\text{T0}}(\text{triclinic leucite}) = 33.2(5)$ GPa, Gatta et al. (2008a); $K_{\text{T0}}(\text{monoclinic wairakite}) = 39(3)$ GPa and $K_{\text{T0}}(\text{triclinic wairakite}) = 24(3)$ GPa, Ori et al. (2008); $K_{\text{T0}}(\text{cubic pollucite}) = 41(2)$ GPa and $K_{\text{T0}}(\text{triclinic pollucite}) = 25.1(9)$ GPa, this study] is not as great as in analcime [$K_{\text{T0}}(\text{cubic analcime}) = 56(3)$ GPa and $K_{\text{T0}}(\text{triclinic analcime}) = 19(2)$ GPa, Gatta et al. (2006)]. In addition, for all the aforementioned isotypic members of the “analcime-group,” the high-to-low symmetry P -induced phase transition is completely reversible.

The adiabatic bulk modulus of the low- P cubic polymorph

of pollucite obtained on the basis of the single-crystal Brillouin scattering experiment [i.e., $K_s = 52.1(10)$ GPa] is significantly higher than the isothermal bulk modulus obtained by static compression in the DAC [i.e., $K_{\text{T0}} = 41(2)$ GPa], even taking into consideration that the isothermal-adiabatic corrections usually amount to about 1–2% at room temperature. The difference between the two bulk moduli is $\sim 5\sigma(K_{\text{T0}})$. Since we used crystals from the same pollucite sample in both experiments (i.e., Brillouin scattering and X-ray diffraction), we believe that the bulk modulus obtained by BM-EoS fit of the P - V data is likely underestimated because of the small P -range investigated (i.e., 0.0001–0.54 GPa, Table 3).

The HP triclinic polymorph of pollucite shows an almost isotropic elastic behavior, as $K_{\text{T0}}(a):K_{\text{T0}}(b):K_{\text{T0}}(c) = 1.10:1:1.09$. This behavior is similar to that observed in triclinic leucite [with $K_{\text{T0}}(a):K_{\text{T0}}(b):K_{\text{T0}}(c) = 1.03:1:1.02$, Gatta et al. (2008a)] but differs significantly from that in triclinic analcime [$K_{\text{T0}}(a):K_{\text{T0}}(b):K_{\text{T0}}(c) = 2.64:1.82:1$]. However, the lack of structural data of the HP triclinic polymorphs of leucite and pollucite hinders an exhaustive discussion on their similar elastic anisotropy, and on the difference with that observed in triclinic analcime.

As already postulated by Gatta et al. (2008a), there is not a simple relationship between ionic radius of the extra-framework cation and transition pressure in the “analcime-group” minerals, because the coordination shells of the extra-framework cations are significantly different [i.e., CsO_{12} - and $\text{NaO}_4(\text{H}_2\text{O})_2$ -polyhedron in low- P pollucite, $\text{NaO}_4(\text{H}_2\text{O})_2$ -polyhedron in low- P analcime; KO_6 in low- P leucite, with the K-sites located at the same positions as the O atoms of the H_2O molecules in analcime; $\text{CaO}_4(\text{H}_2\text{O})_2$ -polyhedron in low- P wairakite, with a configuration similar to that of analcime]. These latest HP experimental findings on pollucite, have led us to reevaluate the role played by the framework (i.e., different Si/Al-distribution, topological symmetry) and extra-framework content (monovalent or divalent cations and water molecules). Neither the ionic radius of the (main) extra-framework cation nor the amount of water plays a significant role on the transition pressure. In contrast, analcime and pollucite share the same symmetry (i.e., cubic) with a fully disordered Si/Al-distribution in the tetrahedral framework, and both show a phase transition at $P \leq 1$ GPa. Leucite is tetragonal with a partial Si/Al-ordering in the framework; its transition pressure is about 2.4 GPa. Wairakite is monoclinic with an ordered Si/Al-distribution; its transition pressure is about 2.5 GPa. It appears, therefore, that the higher the symmetry, the lower the transition pressure. A high symmetry hinders any P -induced structural relaxation, whereas a low symmetry allows the structure to accommodate the effect of pressure with more degrees of freedom. This might explain the low P_T in analcime and pollucite ($Ia\bar{3}d$ at room conditions) and the higher P_T in leucite ($I4_1/a$) and wairakite ($I2/a$).

The high thermo-elastic stability of pollucite, reflected by the preservation of crystallinity at least up to 9 GPa (at room T) and 1470 K (at room P) in elastic regime, the significantly large amount of Cs hosted in this material ($\text{Cs}_2\text{O} \sim 30$ wt%), the immobility of Cs at high-temperature and high-pressure conditions (related to the configuration of the Cs-polyhedron and its bonding environment and to the small dimension of the micropores—“free diameters”—where the Cs-sites lie, $\text{O} \leftrightarrow \text{O}_{6\text{mR}}$, Table 2) and the

extremely low leaching rate of Cs, make of this open-framework silicate a functional material with potential use for fixation and deposition of Cs radioisotopes, as well as a promising solid host for a ^{137}Cs γ -radiation source in sterilization applications (Richerson and Hummel 1972; Gallagher et al. 1977; Komameni and White 1981; Yanagisawa et al. 1987; Mimura et al. 1990; Kobayashi et al. 1997, 2006; Yanase et al. 1997).

ACKNOWLEDGMENTS

High-pressure experiments at the Bayerisches Geoinstitut were performed under the EU "Research Infrastructures: Transnational Access" Program [Contract no. 505320 (RITA)—High Pressure]. This work was also funded by the Italian Ministry of University and Research, MIUR-Project: 2006040119_004. G. Bromiley and an anonymous reviewer, and the Associate Editor M. Kunz, are thanked for their suggestions aimed to improve the quality of the manuscript.

REFERENCES CITED

- Angel, R.J. (2000) Equation of state. In R.M. Hazen and R.T. Downs, Eds., *High-Temperature and High-Pressure Crystal Chemistry*, 41, p. 35–59. Reviews in Mineralogy and Geochemistry, Mineralogical Society of America and Geochemical Society, Chantilly, Virginia.
- (2001) EOS-FIT V6.0. Computer program. Crystallography Laboratory, Department of Geological Sciences, Virginia Tech, Blacksburg.
- (2002) ABSORB V5.2. Computer program. Crystallography Laboratory, Department of Geological Sciences, Virginia Tech, Blacksburg.
- (2003) Automated profile analysis for single-crystal diffraction data. *Journal of Applied Crystallography*, 36, 295–300.
- Angel, R.J., Downs, R.T., and Finger, L.W. (2000) High-temperature—High-pressure diffraction. In R.M. Hazen and R.T. Downs, Eds., *High-Temperature and High-Pressure Crystal Chemistry*, 41, p. 559–596. Reviews in Mineralogy and Geochemistry, Mineralogical Society of America and Geochemical Society, Chantilly, Virginia.
- Angel, R.J., Bujak, M., Zhao, J., Gatta, G.D., and Jacobsen, S.D. (2007) Effective hydrostatic limits of pressure media for high-pressure crystallographic studies. *Journal of Applied Crystallography*, 40, 26–32.
- Armbruster, T. and Gunter, M.E. (2001) Crystal structures of natural zeolites. In D.L. Bish and D.W. Ming, Eds., *Natural Zeolites: Occurrence, Properties, Application*, 45, p. 1–57. Reviews in Mineralogy and Geochemistry, Mineralogical Society of America and Geochemical Society, Chantilly, Virginia.
- Baerlocher, Ch., Meier, W.M., and Olson, D.H. (2001) *Atlas of Zeolite Framework Types*, 5th edition, 302 p. Elsevier, Amsterdam.
- Beger, R.M. (1969) The crystal structure and chemical composition of pollucite. *Zeitschrift für Kristallographie*, 129, 280–302.
- Birch, F. (1947) Finite elastic strain of cubic crystals. *Physical Review*, 71, 809–824.
- Burnham, C.W. (1966) Computation of absorption corrections and the significance of end effect. *American Mineralogist*, 51, 159–167.
- Černý, P. (1974) The present status of the analcime-pollucite series. *Canadian Mineralogist*, 12, 334–341.
- Coombs, D.S., Alberti, A., Armbruster, T., Artioli, G., Colella, C., Galli, E., Grice, J.D., Liebau, F., Mandarino, J.A., Minato, H., Nickel, E.H., Passaglia, E., Peacor, D.R., Quartieri, S., Rinaldi, R., Ross, M., Sheppard, R.A., Tillmanns, E., and Vezzalini, G. (1997) Recommended nomenclature for zeolite minerals: report of the Subcommittee on Zeolites of International Mineralogical Association, Commission on New Minerals and Mineral Names. *Canadian Mineralogist*, 35, 1571–1606.
- Fleischer, M. and Ksanda, C.J. (1940) Dehydration of pollucite. *American Mineralogist*, 25, 666–672.
- Gallagher, S.A., McCarthy, G.J., and Smith, D.K. (1977) Preparation and X-ray characterization of $\text{CsAlSi}_3\text{O}_8$. *Materials Research Bulletin*, 12, 1183–1190.
- Gatta, G.D. (2008) Does porous mean soft? On the elastic behaviour and structural evolution of zeolites under pressure. *Zeitschrift für Kristallographie*, 223, 160–170.
- Gatta, G.D., Nestola, F., and Boffa Ballaran, T. (2006) Elastic behavior, phase transition and pressure induced structural evolution of analcime. *American Mineralogist*, 91, 568–578.
- Gatta, G.D., Rotiroli, N., Boffa Ballaran, T., and Pavese, A. (2008a) Leucite at high-pressure: Elastic behavior, phase stability and petrological implications. *American Mineralogist*, 93, 1588–1596.
- Gatta, G.D., Rotiroli, N., Fisch, M., Kadiyski, M., and Armbruster, T. (2008b) Stability at high-pressure, elastic behavior and pressure-induced structural evolution of $\text{CsAlSi}_3\text{O}_8$, a potential nuclear waste disposal phase. *Physics and Chemistry of Minerals*, 35, 521–533.
- Gottardi, G. and Galli, E. (1985) *Natural Zeolites*, 409 p. Springer-Verlag, Berlin.
- King, H.E. and Finger, L.W. (1979) Diffracted beam crystal centering and its application to high-pressure crystallography. *Journal of Applied Crystallography*, 12, 374–378.
- Kobayashi, H., Yanase, I., and Mitamura, T. (1997) A new model for the pollucite thermal expansion mechanism. *Journal of the American Ceramic Society*, 80, 2161–2164.
- Kobayashi, H., Sumino, S., Tamai, S., and Yanase, I. (2006) Phase transition and lattice thermal expansion of Cs-deficient pollucite, $\text{Cs}_{1-x}\text{Al}_{1-x}\text{Si}_{2+x}\text{O}_6$ ($x \leq 0.25$), compounds. *Journal of the American Ceramic Society*, 89, 3157–3161.
- Komameni, S. and White, W.B. (1981) Stability of pollucite in hydrothermal fluids. *Scientific Basis for Nuclear Waste Management*, 3, 387–396.
- Legache, M. (1995) New experimental data on the stability of the pollucite-analcime series: application to natural assemblages. *European Journal of Mineralogy*, 7, 319–323.
- Mao, H.K., Xu, J., and Bell, P.M. (1986) Calibration of the ruby pressure gauge to 800 kbar under quasi-hydrostatic conditions. *Journal of Geophysical Research*, 91, 4673–4676.
- Mimura, H., Shibata, M., and Akiba, K. (1990) Surface alteration of pollucite under hydrothermal conditions. *Journal of Nuclear Science and Technology*, 27, 835–843.
- Miletich, R., Allan, D.R., and Kush, W.F. (2000) High-pressure single-crystal techniques. In R.M. Hazen and R.T. Downs, Eds., *High-Temperature and High-Pressure Crystal Chemistry*, 41, p. 445–519. Reviews in Mineralogy and Geochemistry, Mineralogical Society of America and Geochemical Society, Chantilly, Virginia.
- Musgrave, M.J.P. (1970) *Crystal Acoustics: Introduction to the Study of Elastic Waves and Vibrations in Crystals*, 288 p. Holden-Day Inc., San Francisco.
- Náray-Szabó, S.V. (1938) Die struktur des pollucits $\text{CsAlSi}_3\text{O}_8 \cdot x\text{H}_2\text{O}$. *Zeitschrift für Kristallographie*, 99, 277–282.
- Newnham, R.E. (1967) Crystal structure and optical properties of pollucite. *American Mineralogist*, 52, 1515–1518.
- Nye, J.F. (1985) *Physical Properties of Crystals. Their Representation by Tensors and Matrices*, 329 p. Oxford University Press, U.K.
- Ogorodova, L.P., Melchakova, L.V., Kiseleva, I.A., and Belitsky, I.A. (2003) Thermochimical study of natural pollucite. *Thermochimica Acta*, 403, 251–256.
- Ori, S., Quartieri, S., Vezzalini, G., and Dmitriev, V. (2008) Pressure-induced structural deformation and elastic behavior of wairakite. *American Mineralogist*, 93, 53–62.
- Palmer, D.C., Dove, M.T., Ibberson, R.M., and Powell, B.M. (1997) Structural behavior, crystal chemistry, and phase transitions in substituted leucite: High-resolution neutron powder diffraction studies. *American Mineralogist*, 82, 16–29.
- Richerson, D.W. and Hummel, F.A. (1972) Synthesis and thermal expansion of polycrystalline cesium minerals. *Journal of the American Ceramic Society*, 55, 269–273.
- Sanchez-Valle, C., Sinogeikin, S.V., Lethbridge, Z.A.D., Evans, K.E., and Bass, J.D. (2005) Brillouin scattering study on the single-crystal elastic properties of natrolite and analcime zeolites. *Journal of Applied Physics*, 98, 053508.
- Sanchez-Valle, C., Lethbridge, Z.A.D., Sinogeikin, S.V., Williams, J.J., Walton, R.I., Evans, K.E., and Bass, J.D. (2008) Negative Poisson's ratios in MFI-silicalite zeolites. *Journal of Chemical Physics*, 128, 184503.
- Sandercock, J.R. (1982) Trends in Brillouin scattering: studies of opaque materials, supported films, and central modes. In M. Cardona and G. Güntherodt, Eds., *Topics in Applied Physics*, 51, p. 173–206. Springer, Berlin.
- Sheldrick, G.M. (1997) *SHELX-97. Programs for crystal structure determination and refinement*. University of Göttingen, Germany.
- Taylor, D. and Henderson, C.M.B. (1968) The thermal expansion of the leucite group of minerals. *American Mineralogist*, 53, 1476–1489.
- Teertstra, D.K. and Černý, P. (1995) First natural occurrences of end-member pollucite: A product of low-temperature reequilibration. *European Journal of Mineralogy*, 7, 1137–1148.
- Wilson, A.J.C. and Prince, E. (1999) *International Tables for X-ray Crystallography, Volume C: Mathematical, Physical, and Chemical Tables* (2nd edition). Kluwer Academic, Dordrecht.
- Xu, H., Navrotsky, A., Balmer, M.L., and Su, Y. (2002) Crystal chemistry and phase transitions in substituted pollucites along the $\text{CsAlSi}_3\text{O}_8$ - $\text{CsTiSi}_2\text{O}_6$ join: A powder synchrotron X-ray diffraction study. *Journal of the American Ceramic Society*, 85, 1235–1242.
- Yanagisawa, K., Nishioka, M., and Yamasaki, N. (1987) Immobilization of cesium into pollucite structure by hydrothermal hot-pressing. *Journal of Nuclear Science and Technology*, 24, 51–60.
- Yanase, I., Kobayashi, H., Shibasaki, Y., and Mitamura, T. (1997) Tetragonal-cubic structural phase transition in pollucite by low-temperature X-ray powder diffraction. *Journal of the American Ceramic Society*, 80, 2693–2695.

MANUSCRIPT RECEIVED JANUARY 14, 2009

MANUSCRIPT ACCEPTED APRIL 17, 2009

MANUSCRIPT HANDLED BY MARTIN KUNZ